Analytica Chimica Acta 936 (2016) 83–90

Contents lists available at ScienceDirect

Analytica Chimica Acta

journal homepage: www.elsevier.com/locate/aca

Titania nanotubes decorated with gold nanoparticles for electrochemiluminescent biosensing of glycosylated hemoglobin

Qun Zhao [a, b], Shan Tang [a], Chen Fang [a, c, **], Yi-Feng Tu [a, *]

[a] Institute of Analytical Chemistry, Dushu Lake Campus, Soochow University, Industrial Park, Suzhou, 215123, PR China
[b] College of Chemistry and Chemical Engineering, Nantong University, Nantong, 226019, PR China
[c] Second Affiliated Hospital, Soochow University, Suzhou, 215004, PR China

HIGHLIGHTS

- The enhanced electrochemiluminescence of luminol by AuNPs/TiNTs.
- An ECL biosensor for HbA1c assay with ultra-high sensitivity.
- A promising disposable device for diabetic diagnosis and treatment even for POCT.
- The excellent regression of detected results with gold-standard method.

GRAPHICAL ABSTRACT

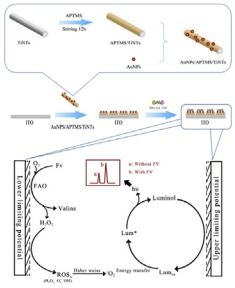

ARTICLE INFO

Article history:
Received 30 April 2016
Received in revised form
1 July 2016
Accepted 11 July 2016
Available online 16 July 2016

Keywords:
Electrochemiluminescence
Luminol
AuNPs/TiNTs
Glycosylated hemoglobin
Fructosyl amino-acid oxidase

ABSTRACT

A glycated hemoglobin (HbA1c) biosensor with high performance has been constructed in this work. Here the fructosyl amino acid oxidase was immobilized onto a pre-functionalized indium tin oxide glass with titania nanotubes decorated with gold nanoparticles. The property of nanocomposite was characterized by transmission electromicroscopy, scanning electron microscopy, electrochemistry and spectroscopy. Under the optimum conditions, fructosyl valine was detected by this biosensor. It exhibited a linear detection range from 4.0×10^{-9} M to 7.2×10^{-7} M, and a limit of detection for 3.8×10^{-9} M at the signal-to-noise ratio of 3. Thus the HbA1c level in whole blood samples of healthy individuals or diabetic patients were evaluated with designed biosensor after pre-treatment of hydrolysis. The results of our detection were closely consistent with that of the standard method. At the same time, our biosensor has some advantages including high sensitivity, disposable usage and low cost, which implies its great promising application in point-of-care testing of HbA1c.

© 2016 Elsevier B.V. All rights reserved.

1. Introduction

The 2014 report of International Diabetes Federation (IDF) has pointed out that 8.2% (about 387 millions) of adults (aged from 20 to 79) were suffered from diabetes mellitus worldwide, and still in ever-increasing rapidly [1]. Diabetes mellitus is a chronic metabolic disease characterized by high blood glucose. Diabetes itself does not affirmatively result in severe harm to patients, but a chronic high blood glucose level will lead to dangerous syndromes for heart, brain, blood vessels, eyes, kidneys, feet, peripheral nerves, teeth and so on. According to the report of WHO, there are more than 100 kinds of complications of diabetes [2–4]. Also the diabetic patients have higher risk of infections from bacteria or virus.

* Corresponding author.
** Corresponding author. Institute of Analytical Chemistry, Dushu Lake Campus, Soochow University, Industrial Park, Suzhou, 215123, PR China.
E-mail address: tuyf@suda.edu.cn (Y.-F. Tu).

http://dx.doi.org/10.1016/j.aca.2016.07.015
0003-2670/© 2016 Elsevier B.V. All rights reserved.

Conclusively, diabetes mellitus has already been proved to be a global public health issue. In a representative sample, the prevalence of diabetes of Chinese adults has exceeded 10%, which shares in the greatest portion of diabetic patients in the world [5–7].

The blood glucose index [8] reflects an immediate fluctuating glucose level, but it is easily disturbed by daily diet thus requires frequent measurements. Another more useful diagnostic marker, glycated hemoglobin (HbA1c), an irreversible coalition of hemoglobin with D-glucose via the N-terminal group of its β-chain, is accepted as a months-long standard of diabetic condition [9–14]. Not only related to the concentration of blood glucose, the HbA1c index reflects the average blood glucose level during past 2–3 months without fluctuation since it has a half-life time of 7–8 weeks [15]. This is the most beneficial feature of HbA1c assay for diabetes diagnosis and treatment.

Currently, the methods include high-performance liquid chromatography (HPLC), electrophoresis, electroendosmosis, ion exchange chromatography, boronate affinity chromatography, isoelectric focusing method, immunoassay, liquid chromatography-tandem mass spectroscopy, fluorometry, colorimetry and so on have been applied for clinical HbA1c assay [12]. Among them, HPLC is generally accepted as the gold standard method. But these methods require expensive equipments, complex operation, consuming time, high cost and trained persons to operate. And there are multiple controversies due to the discrepancy on precision and accuracy between various commercial methods [16]. The development of portable HbA1c testing device, with high accuracy, simple/convenient operation and low cost, is still in broad promising application and also has high commercial value.

Nowadays, the electrochemical biosensors have been proved to be a kind of widespread, multitudinous and gradually commercialized devices. The matrix of electrochemical biosensors always include a biological recognition element to ensure its unique identification and high selectivity towards target molecule. They are widely used in chemistry, biology, food safety, environmental monitoring, pharmaceutical or clinical laboratories and so on [11]. Recently, considering the possibility to overcome those mentioned limitations of the methods for HbA1c assay, the electrochemical biosensor profiles a bright future. The prominent advantages of electrochemical biosensor for HbA1c generally including miniaturized size, portability and convenient usage make it most likely succeeding in clinical point-of-care testing (POCT) [16–18]. But, only few reports have focused on it until now.

There are two categories of electrochemical HbA1c biosensor known as the enzyme sensor [19–24] (based on detection of fructosyl valine (FV) under the catalysis of fructosyl amino-acid oxidase, FAO) or immunosensor [25–28]. The advantages of enzymatic method include good reliability, high sensitivity and relatively fast response. The principle for HbA1c assay is supposed to consist of following steps:

$$\underset{\text{(N-terminal residue of b-chain in HbA1c)}}{\text{HbA1c}}\xrightarrow{\text{endoproteinase Glu.C}}\text{Fru-Val-His-Leu-Thr-Pro-Glu-Glu-Lys-ser}\ldots \quad (1)$$

$$\underset{\text{(N-terminal residue of b-chain in HbA1c)}}{\text{Fru-Val-His-Leu-Thr-Pro-Glu-Glu-Lys-ser}\ldots}\xrightarrow{\text{Protease}}\underset{\text{(FV)}}{\text{Fructosyl valine}}+\underset{\text{(His, Leu, Thr)}}{(\text{amino acid})_{n-1}} \quad (2)$$

$$\text{FV}+\text{O}_2+\text{H}_2\text{O}\xrightarrow{\text{FAO}}\text{Valine}+\text{D-glucose}+\text{H}_2\text{O}_2 \quad (3)$$

The electrochemiluminescent (ECL) analysis is an attractive method owing to its high sensitivity, good controllability, simplicity, rapidity, and low cost [29–31]. Because of the non-toxicity, cheapness, and high light-emitting quantum yield, luminol is one of the most significant luminophore and has been used in ECL detection of some biomarkers [32–35]. The HbA1c in blood samples will be transformed into FV during the enzymolysis, and thereafter to be oxidized under the catalysis of FAO. As one of the reactive oxygen species (ROSs), the co-produced H_2O_2 of this reaction will greatly intensify the ECL of luminol [36,37]. But, as far as we know, no related work about ECL enzyme sensor for HbA1c has been reported yet.

Series of specially structured nanosized titania, as nanotubes, arrayed nanotubes, nanobelts, nanowires or nano-rods have been prepared and applied in a lot of important researches because of their outstanding performance [38–41]. We have also synthesized and intensively studied the application of hollowed titania nanoshell (HTNSs) [42] and titania nanotubes (TiNTs) [43] in ECL analysis with luminol as a luminophore. These two materials can promote the redox of hydrogen peroxide, to further increase the ECL of luminol and greatly promote the sensitivity of H_2O_2 detection. Also as we all know, AuNPs have a large specific surface area, excellent electrical conductivity and good biocompatibility, it also can promote the ECL of luminol [44]. In recent years, we have also reported some modified electrodes of TiO_2 and AuNPs or AuAg alloy nanocomposite for enhancement of the luminol ECL [45,46].

In this work, we successfully prepared an Au/TiNTs nanocomposites by the means of physical/chemical functions of (3-aminopropyl)trimethoxysilane (APTMS). Then it was covered on an indium tin oxide (ITO) glass together with cross-linked FAO to acts as a sensing matrix for ECL detection of FV in pretreated blood sample. It is known that two FV molecules would be released during the protease digestion from one HbA1c molecule, thus a quantitative relation toward HbA1c is established and therefore the HbA1c level (HbA1c %) can be calibrated as the ratio of glycated hemoglobin to total hemoglobin. Compare with other current testing methods, including electrochemical methods, the fabricated ECL sensor showed a higher sensitivity, lower detection limit, good reliability and faster implementation. The design of this new sensor is not only to simply assemble those materials and signaling technic together, but also to deeply exploit the potentiality of synergic effect between those nano-materials themselves, the ROSs from enzymatic reaction and the electrolysis induced redox to trigger stronger light-emission of luminol which proportionally related to the concentration of substrate. This is a sole report about the ECL biosensor for HbA1c with highest sensitivity but equally simple preparation/operation.

2. Experimental

2.1. Materials and reagents

(3-aminopropyl)trimethoxysilane (APTMS) was purchased from Aladdin Industrial Co. Ltd. (Shanghai, P.R. China). $HAuCl_4 \cdot 4H_2O$ were purchased from Sinopharm Chemical Reagent Co. Ltd. (Shanghai, P.R. China). TiO_2 powder (P-25) was purchased from Degussa Co. Ltd. (Germany). Luminol were obtained from Fluka Chemical Co. Ltd. (USA). Fructosyl-amino acid oxidase (FAO, 5.4 U mg^{-1}) was purchased from Beijing Springup Scientific Co. Ltd. (Beijing, P.R. China). FV was procured from Toronto Research Chemicals Inc. (Canada). Phosphate buffer solution (0.2 M) were prepared by varying the ratio of NaH_2PO_4 to Na_2HPO_4 and NaOH. All of the other chemicals were obtained from Chemical Reagent Company of Shanghai (Shanghai, P.R. China). All of the chemicals were analytical grade and used without further purification. ITO glass was purchased from Suzhou Nippon Sheet Glass Electronics Co. Ltd. (Suzhou, PR China). Ultrapure water (ALH-6000-U ultrapure water system, Aquapro, P.R. China) was used throughout the experiments.

2.2. Apparatus and instruments

The ECL analysis is carried out on our lab-built installation. A three-electrode system, including a bare or functionalized ITO glass (1 cm × 5 cm) as the working electrode, a platinum wire as auxiliary electrode and a silver wire as reference electrode, was employed. The micromorphology and the size of TiNTs, AuNPs, Au/TiNTs and fabricated electrodes were observed by scanning electron microscopy (S-4700 scanning electron microanalyzer, Hitachi, Japan) and high resolution transmission electron microscopy (G220, at an accelerating voltage of 200 KV, FEI, USA). The electrochemical experiments were carried out on a CHI 800 Electrochemical Workstation (ChenHua Instrument Co. Ltd., Shanghai, P.R. China). The UV–Vis absorption spectra were obtained with a 2810 UV–Vis spectrophotometer (Hitachi, Japan). Centrifugal treatment was carried on an Allegra 64R Centrifuge (Beckman Coulter, USA). The blood samples of healthy volunteers and diabetics were obtained from Second Affiliated Hospital of Soochow University, with EDTA as anticoagulant, and reserved at 4 °C. The standard HbA1c values of those samples were determined by Alere Afinion AS100 Analyzer (Alere Inc., USA).

2.3. The preparation of Au/TiNTs nanocomposite

TiNTs were synthesized by a hydrothermal method consulted to previous reports [47,48]. AuNPs with about 5 nm of diameter were prepared following a typical procedure [49]. The Au/TiNTs nanocomposite were prepared referring to the literature [50]. The first is to attach a polymer layer on TiNTs by the hydrolysis of APTMS. 0.05 g of TiNTs was dispersed into 20 mL of ethanol in a beaker equipped with magnetic agitator, followed by addition of 200 μL of APTMS and 4 mL of 7.5 M ammonia. After 12 h, the solid was centrifugal separated and rinsed for 4 times with ethanol and water, and finally dispersed them in 10 mL of ultrapure water. Under the sonication, the AuNPs was mixed in, and kept the agitation for 30 min, then centrifuged and washed for 3 times with distilled water. Finally, dispersed them in 400 μL of ultrapure water for further use.

2.4. The preparation of Au/TiNTs/ITO electrode

Pieces of ITO glass were cut into 1 cm × 5 cm, and then treated in sequence under ultrasonication with water, ethanol/1 M NaOH (1:1, v/v), acetone and water for 15 min each. After dried with nitrogen-blowing, certain volume of Au/TiNTs suspension was cast onto it, then dried under infrared lamp.

2.5. The preparation of biosensor (FAO/Au/TiNTs/ITO)

The glutaraldehyde (GA, 0.25 wt%), bovine serum albumin (BSA,

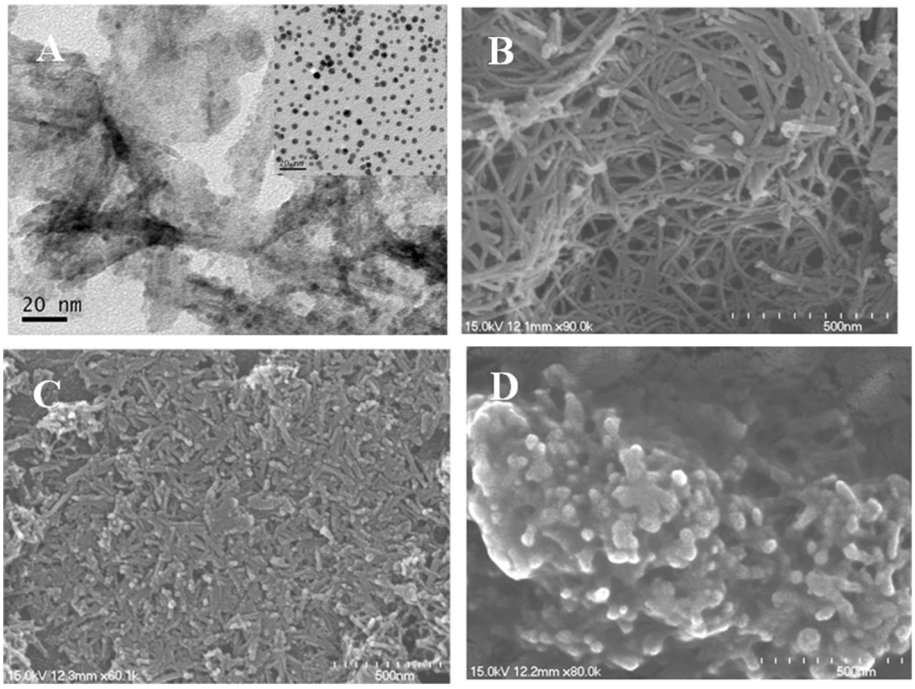

Fig. 1. (A) The TEM image of AuNPs/TiNTs, here the inset is the picture of AuNPs; (B) the SEM image of TiNTs/ITO; (C) the SEM image of AuNPs/TiNTs/ITO; (D) the SEM image of resultant biosensor.

0.5 mg mL^{-1}) and FAO (30 U mL^{-1}) were well mixed together (all of these materials were dissolved in phosphate buffer, pH = 7.0), then dropped onto an Au/TiNTs/ITO electrode with 5 μL of total amount. The biosensor was accomplished after the finish of cross-linking reaction during a period of quiescence in a refrigerator at 4 °C.

2.6. The optimisation of important factors of ECL measurements

All electrochemical characterization and measurements were carried out using a conventional three-electrode system with the sensor as working electrode, a Pt wire as auxiliary electrode, and an Ag wire as reference electrode. The volume of detection cell is 5 mL. The fittest acidity for FAO activity is around pH 6.0, but the signal of luminol ECL is very weak in this pH. Considering the counterbalance between enzyme activity and the condition for luminol ECL, pH = 8.0 was decided as the best selection. At the same time, in order to facilitate the experimental operation and the feasibility of POCT device, the ambient temperature (25 °C) was chosen as the experimental condition.

We optimised all of the parameters that strongly influenced the ECL performance of luminol. First of all, concerned the basal electrode, Au/TiNTs/ITO, including the mass ratio of TiNTs to AuNPs, the usages of AuNPs, the dosage of APTMS and the used amount of Au/TiNTs, were all optimised. Next, the dosage of FAO, the concentration of cross-linking matrix (GD, BSA), the employed volume of matrix were investigated too. At the same time, the detection conditions such as upper/lower limiting potential and pulse period were also optimised.

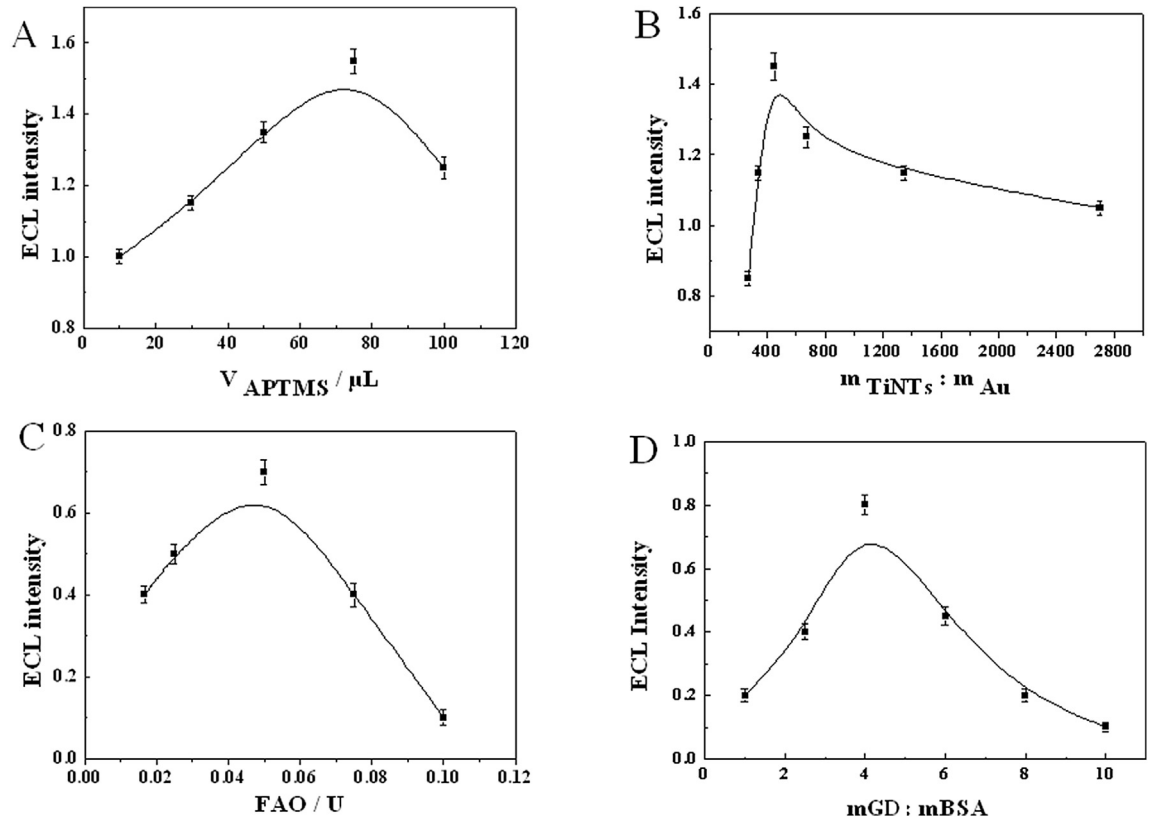

Fig. 2. The effects of biosensor components on ECL response of (A) the volume of APTMS; (B) the mass ratio of TiNTs to AuNPs; (C) the usage of FAO; (D) the mass ratio of GD to BSA.

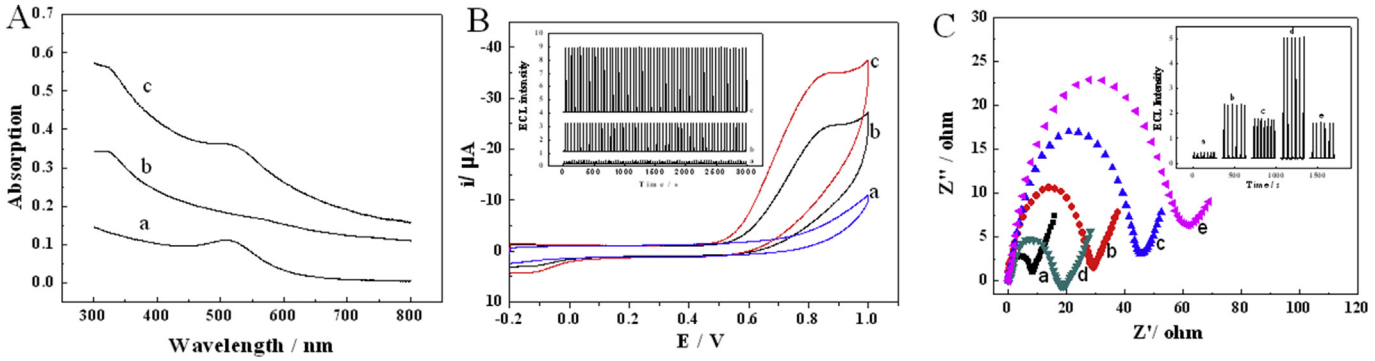

Fig. 3. (A) The UV–vis absorption spectra of (a) AuNPs, (b) TiNTs and (c) Au/TiNTs; (B) the cyclic voltammograms of 0.1 mM luminol on (a) bare ITO, (b) TiNTs/ITO and (c) AuNPs/TiNTs/ITO in buffer solution of pH 8.0 at a scan rate of 50 mV s^{-1}; here the inset is the real map of the ECL signal correspondingly and (C) the electrochemical impedance spectroscopy of (a) bare ITO, (b) TiNTs/ITO, (c) APTMS/TiNTs/ITO, (d) AuNPs/APTMS/TiNTs/ITO and (e) the resultant biosensor, in 0.1 M KCl solution containing 5 mM $[Fe(CN)_6]^{3-}$, inserted is the real maps of corresponding ECL signals.

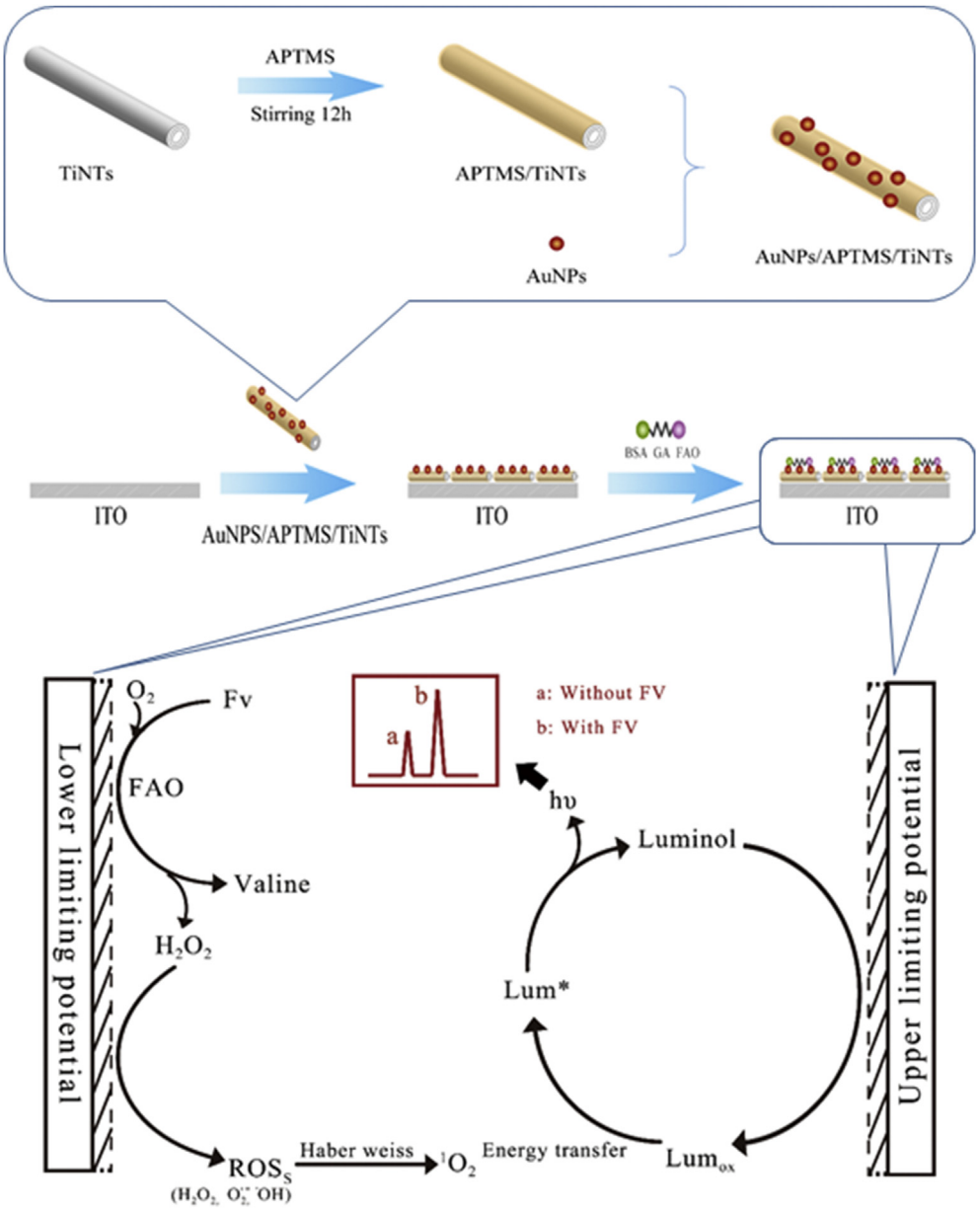

Scheme 1. The preparing procedure of the biosensor and the sensing mechanism.

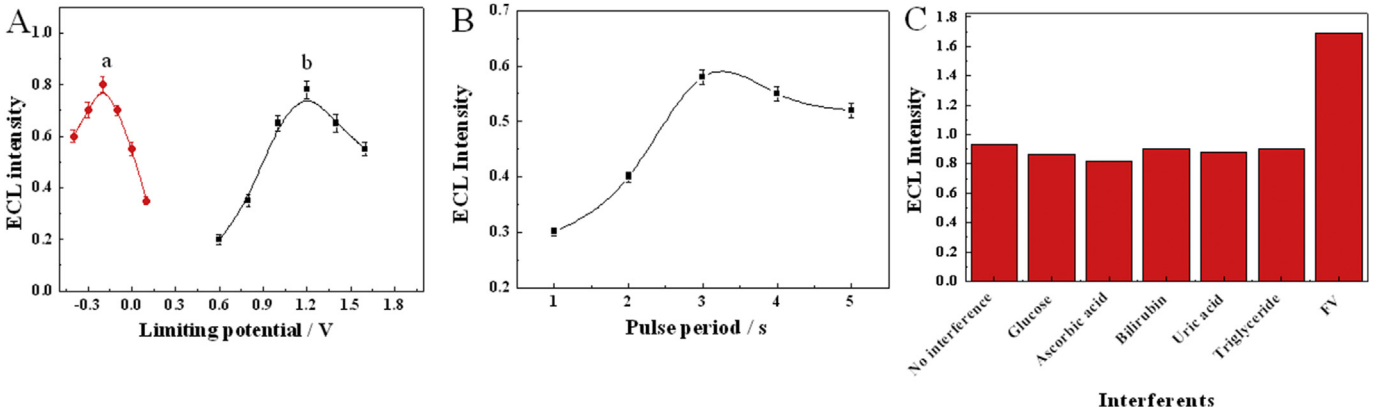

Fig. 4. The effects of experimental parameters on ECL response of (A) lower limiting potential (a) and upper limiting potential (b) and (B) the pulse period. (C) The disturbing degrees of potential interferents.

2.7. The detection of HbA1c in whole blood samples by the biosensor

Before the HbA1c testing, the whole blood samples will be pretreated following the instruction of enzyme kit (Afinion®). Under the optimal conditions, the HbA1c test was carried on with FV as the calibration standard. Thus the HbA1c % value was calculated as the ratio of HbA1c (mM) toward total hemoglobin (mM) which was obtained from the hospital laboratory. Finally, the results were compared with that obtained by the standard immunoassay method using Alere Afinion AS100 Analyzer.

3. Results and discussion

3.1. The characterization of prepared Au/TiNTs and resultant biosensor

3.1.1. The morphology of nano-materials and sensor

The structure and morphology of Au/TiNTs hybrid nanomaterial were characterized by TEM, showed in Fig. 1A. The image clearly demonstrates that the TiNTs present as the form of long and hollow nanotubes with the inner diameter of about 10 nm and an outer diameter of approximately 20 nm. In addition, it can be observed that the diameter of the AuNPs is about 5 nm and attached uniformly on the surface of the TiNTs. The insert in Fig. 1A is the enlarged TEM of AuNPs, which presents its uniform size and distribution.

APTMS plays a key role in the preparation of Au/TiNTs nanocomposites. After rapid hydrolysis, APTMS quickly forms a thin polymer film, and the surface of TiNTs is wrapped by the film through physical embedding. The $-NH_2$ groups of APTMS acts as the linker provided the hydrogen bond and metal-ligand bond for junction of AuNPs. At the same time, the methoxy groups of ATPMS turned into hydroxyl groups after hydrolysis, then combined with the hydroxyl groups of TiNTs on its surface. To summarize, APTMS expresses dual functions of physical embedding and chemical bonding, ensured tightly decoration of AuNPs uniformly on the surface of the TiNTs.

The surface morphologies of TiNTs/ITO, Au/TiNTs/ITO, and resultant sensor were observed using SEM. The TiNTs shows its loosely intertwined structure with the length of several hundreds of nanometre (Fig. 1B). The SEM image of the Au/TiNTs/ITO also exhibits the tubular TiNTs and attached dots of AuNPs (Fig. 1C). The surface of resultant sensor appears as a glutinous paste after immobilizing FAO, showed in Fig. 1D, demonstrated the formation of the sensing matrix.

3.1.2. The optimisation of the biosensor fabrication

According to the previous discussion, immoderately thick film of hydrolyzed APTMS on TiNTs will impede the electron transfer thereafter to restrain the ECL of luminol, but less amount of APTMS is not conducive to AuNPs attachment on the surface of TiTNs. To mostly take the effect of the TiNTs and AuNPs to get maximized ECL, there must be a suitable usage of APTMS. Fig. 2A shows that the optimal volume of APTMS was 75 μL. The usage of AuNPs also affects the performance of ECL, as shown in Fig. 2B, the optimal mass ratio of TiNTs to AuNPs is about 675:1.

As can be seen from Fig. 2C, the ECL intensity increased at first then decreased afterward along with the increasing FAO dosage. The ECL intensity reached to maximum at the actual dosage of 0.05U FAO. As a coupling agent and enzyme stabilizer [51–53], the mass ratio of GD to BSA was optimised as 4:1 (see Fig. 2D).

3.1.3. The spectrometric and electrochemical properties of nanocomposite

The formation of Au/TiNTs nanocomposite was confirmed by UV–Vis absorption spectra in Fig. 3A. Compared with pure TiNTs (curve b), the AuNPs (curve a) and Au/TiNTs (curve c) display the typical absorbance band at 515 nm obviously, confirm the existence of AuNPs.

Fig. 3B represents the cyclic voltammograms (CV) of 0.1 mM luminol on bare ITO, TiNTs/ITO or Au/TiNTs/ITO in buffer solution. As we can see, no oxidation peak can be observed on curve a, but a very clear oxidation peak emerged around the potential of 0.8V on curve b, and a further increased peak on curve c. Meanwhile the ECL signal of 0.1 mM luminol on those electrode are inserted in Fig. 3B, which was totally consistent with the result of CV. These results strongly support our previous discussions about the ECL enhancing mechanism of luminol [36,37,54] and the acceleration of the oxygen reduction to yield the $^1O_2$ which boost the excitation of luminol [42,43,45] by those nanomaterials of metals or their oxide (MONPs), as illustrated in Scheme 1.

The electrochemical impedance spectroscopy (EIS) had been employed to investigate the change of impedance of the electrode when FAO was immobilized on. As we can see from Fig. 3C, the bare ITO electrode (curve a) has small degree of semicircle domain, while that of the TiNTs/ITO (curve b) become larger because of the largish electron transfer resistance of TiNTs. When APTMS/TiNTs were coated on the ITO, the electron transfer resistance increased dramatically (curve c). Then, Au/APTMS/TiNTs/ITO (curve d) exhibited a significant decrease of the electron transfer resistance, which must be attributed to the excellent electrical conductivity of AuNPs. Finally, curve e (FAO/Au/APTMS/TiNTs/ITO) showed an

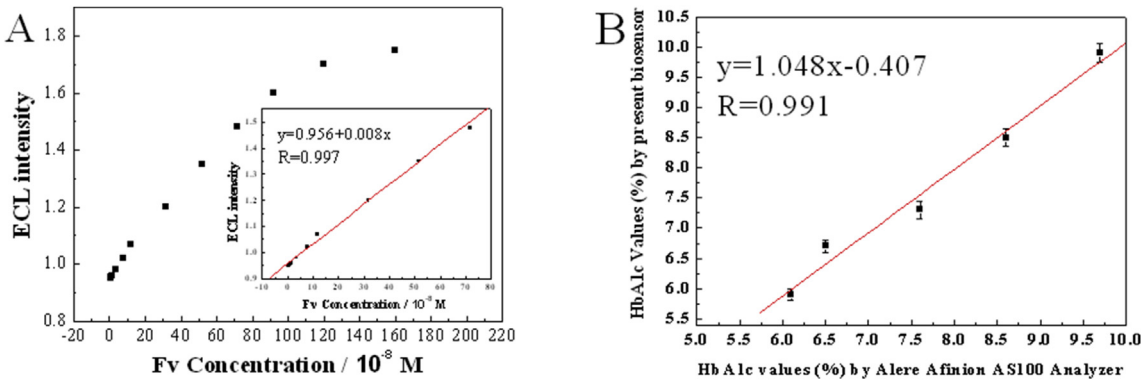

Fig. 5. (A) The output of the biosensor upon FV concentration in buffered solution (pH 8.0), here the inset is the linearity of ECL response; (B) the correlation between the determined results of HbA1c % level by immunoassay (x) and developed biosensor (y).

Table 1
The comparison of present biosensor with reported biosensors.

Types of biosensor	Linear range	Detection limit (S/N = 3)	Ref.
FAO/MNPs/Au	0–2 mM	0.1 mM	[9]
FAO/ZnONPs/Au	0.1–3.0 mM	50 μM	[10]
iridium-modified SPE	0–500 μM	–	[11]
FAO/PVA–SbQ/glass plate	0.2–10 mM	0.2 mM	[12]
carbon paste electrode	0–1 mM	0.05 mM	[14]
FAO/Au/TiNTs/ITO	4.0×10^{-9} M–7.2×10^{-7} M	3.8×10^{-9} M	Present work

obviously increased diameter when FAO was immobilized on, because the enzyme layer obstructed the electron transfer. The insert here displays the ECL signals of 0.1 mM luminol on those electrodes, clearly reflects the variation of ECL performance along with the surface alteration.

3.2. The optimisation of analytical conditions

The ECL intensity relates to the potential and period of pulsed electrolytic power. For consideration of the signal/noise ratio, it is clear that the maximum ECL intensity appeared at −0.2 V of lower limiting potential and 1.3 V of upper limiting potential, showed in Fig. 4A. Furthermore, Fig. 4B demonstrates the optimal pulse period of 3 s.

The interference of several possible interfering substances on the biosensor were investigated, such as 1×10^{-4} M triglycerides, 1×10^{-4} M glucose, 1×10^{-5} M ascorbic acid, 1×10^{-4} M bilirubin and 1×10^{-4} M uric acid. There were tiny degrees of quenched ECL intensity from them (see Fig. 4C), just opposite to the enhancing effect of FV with an equivalence of far larger than 200 of tolerances. The results demonstrate a high selectivity of prepared biosensor toward FV.

3.3. The evaluation of biosensor for FV and blood determination

Under the optimised experimental conditions, the ECL output of resultant sensor upon subsequent addition of different concentrated FV was recorded as shown in Fig. 5A within the concentration range from 4.0×10^{-9} M to 1.6×10^{-6} M. The ECL signal increased linearly along with the concentration of FV, but gradually slow-down when the FV concentration reach a certain level. There is a linear regression between ECL intensity and FV concentration within the range from 4.0×10^{-9} M to 7.2×10^{-7} M (shown as the insert in Fig. 5A) with a detection limit of 3.8×10^{-9} M (S/N = 3). Here, Table 1 lists the performance for FV detection by some other enzyme sensors. It is so clear that the present biosensor is one of the most sensitive ones among them. To determine the repeatability of the resultant biosensor, 5.0×10^{-7} M FV was investigated for three times by single sensor successively. The relative standard deviation is 2.2%, which implied a rather good precision.

The accuracy of the present method was tested by comparing HbA1c values in 5 whole blood samples using present sensor (y) with those obtained by standard method (x), which was proceed by Alere Afinion AS100 Analyzer (immunoassay method). The values obtained in two methods showed a good correlation with a regression coefficient of 0.991 (Fig. 5B), which demonstrated adequate reliability of our sensor. The recovery tests were conducted using standard addition method with the results in Table 2, ranged in 90.5%–103%, which indicated a good accuracy of the biosensor.

Table 2
The recoveries of FV determination.

Sample no.	FV in blood (10^{-8} M)	Added (10^{-8} M)	Found (10^{-8} M)	Recovery (%)	RSD (%, n = 5)
1	7.65	2	9.46	90.5	2.85
2	11.9	10	22.2	103	3.05
3	20.4	30	48.6	94.0	2.95

3.4. The stability of the biosensor

The long-term stability of the biosensor was evaluated over 20 days by monitoring the ECL response upon 5.0×10^{-7} M FV under the optimised conditions. The activity of the sensor remains above 97% of its initial value after 10 days and 95% for 20 days when it was stored at 4 °C. The reproducibility of the biosensor was also investigated by the detection of 5.0×10^{-7} M FV with five parallel biosensors. The relative standard deviation were 4.5%, which implied a commendable performance.

4. Conclusion

A novel ECL biosensor for HbA1c has been prepared, based on immobilization of FAO onto an Au/TiNTs nano-functionalized ITO. This disposable, low-cost biosensor is applicable for the detection of HbA1c by monitoring the produced FV during its enzymolysis. The sensor shows high sensitivity than other reported enzymatic biosensors, and also exhibits enough stability and accuracy. It is in great promising of use in the diagnosis and management of diabetic patients.

Acknowledgments

This work is financially supported by the National Natural Science Foundation of China (21175096, 21375091).

References

[1] J.D.R. Fernandes, K. Ogurtsova, U. Linnenkamp, L. Guariguata, T. Seuring, P. Zhang, D. Cavan, L.E. Makaroff, IDF Diabetes Atlas estimates of 2014 global health expenditures on diabetes, Diabetes Res. Clin. Pract. 117 (2016) 48–54.
[2] C.P. Domingueti, L.M.S. Dusse, M.D.G. Carvalho, L.P.D. Sousa, K.B. Gomes, A.P. Fernandes, Diabetes mellitus: the linkage between oxidative stress, inflammation, hypercoagulability and vascular complications, J. Diabetes Complicat 30 (2016) 738–745.
[3] R.K. Sayyid, N.E. Fleshner, Diabetes mellitus type 2: a driving force for urological complications, Trends Endocrin. Me 27 (2016) 249–261.
[4] K.E. Rollins, K.K. Varadhan, K. Dhatariya, D.N. Lobo, Systematic review of the impact of HbA1c on outcomes following surgery in patients with diabetes mellitus, Clin. Nutr. 35 (2016) 308–316.
[5] D.R. Whiting, L. Guariguata, C. Weil, J. Shaw, IDF Diabetes Atlas: global estimates of the prevalence of diabetes for 2011 and 2030, Diabetes Res. Clin. Pract. 94 (2011) 311–321.
[6] L.N. Huang, L.Y. Yang, X.M. Shen, S.J. Yan, Relationship between glycated hemoglobin A1c and cognitive function in nondemented elderly patients with type 2 diabetes, Metab. Brain Dis. 31 (2016) 347–353.
[7] Y. Xu, L.M. Wang, J. He, Y. Bi, M. Li, T.G. Wang, L.H. Wang, Y. Jiang, M. Dai, J.L. Lu, M. Xu, Y.C. Li, N. Hu, J.H. Li, S.Q. Mi, C.S. Chen, G.W. Li, Y.M. Mu, J.J. Zhao, L.Z. Kong, J.L. Chen, S.H. Lai, W.Q. Wang, W.H. Zhao, G. Ning, Prevalence and control of diabetes in chinese adults, Jama 310 (2013) 948–959.
[8] R.J. Koenig, C.M. Peterson, R.L. Jones, C. Saudek, M. Lehrman, A. Cerami,

Correlation of glucose regulation and hemoglobin AIc in diabetes mellitus, N. Engl. J. Med. 295 (1976) 417–420.
[9] D.E. Goldstein, R.R. Little, R.A. Lorenz, J.I. Malone, D. Nathan, C.M. Peterson, D.B. Sacks, Tests of glycemia in diabetes, Diabetes Care 27 (2004) 1761–1773.
[10] W.G. John, Haemoglobin A1c reference method, Scand. J. Clin. Lab. Invest. 66 (2006) 1–4.
[11] E.S. Kilpatrick, HbA1c measurement, J. Clin. Pathol. 57 (2004) 344–345.
[12] S. Yazdanpanah, M. Rabiee, M. Tahriri, M. Abdolrahim, L. Tayebi, Glycated hemoglobin-detection methods based on electrochemical biosensors, Trac-Trend Anal. Chem. 72 (2015) 53–67.
[13] C.S. Pundir, S. Chawla, Determination of glycated hemoglobin with special emphasis on biosensing methods, Anal. Biochem. 444 (2014) 47–56.
[14] S.H. Ang, M. Thevarajah, Y. Alias, S.M. Khor, Current aspects in hemoglobin A1c detection: a review, Clin. Chim. Acta 439 (2015) 202–211.
[15] A. Diabet, Standards of medical care in diabetes-2011 american diabetes association, Diabetes Care 34 (2011) S11–S61.
[16] A.S. Hwang, M. Thevarajah, A. Yatimah, K.S. Mei, Current aspects in hemoglobin A1c detection: a review, Clin. Chim. Acta 439 (2015) 202–211.
[17] B.Z. Wang, J.I. Anzai, Recent progress in electrochemical HbA1c sensors: a review, Materials 8 (2015) 1187–1203.
[18] C.S. Pundir, S. Chawla, Determination of glycated hemoglobin with special emphasis on biosensing methods, Anal. Biochem. 444 (2014) 47–56.
[19] Y. Nanjo, R. Hayashi, T. Yao, An enzymatic method for the rapid measurement of the hemoglobin A1c by a flow-injection system comprised of an electrochemical detector with a specific enzyme-reactor and a spectrophotometer, Anal. Chim. Acta 583 (2007) 45–54.
[20] L. Fang, W. Li, Y. Zhou, C.C. Liu, A single-use, disposable iridium-modified electrochemical biosensor for fructosyl valine for the glycoslated hemoglobin detection, Sensors Actuat. B-Chem. 137 (2009) 235–238.
[21] S. Chawla, C.S. Pundir, An electrochemical biosensor for fructosyl valine for glycosylated hemoglobin detection based on core-shell magnetic bionanoparticles modified gold electrode, Biosens. Bioelectron. 26 (2011) 3438–3443.
[22] S. Chawla, C.S. Pundir, An amperometric hemoglobin A1c biosensor based on immobilization of fructosyl amino acid oxidase onto zinc oxide nanoparticles-polypyrrole film, Anal. Biochem. 430 (2012) 156–162.
[23] K. Ogawa, D. Stollner, F. Scheller, A. Warsinke, F. Ishimura, W. Tsugawa, S. Ferri, K. Sode, Development of a flow-injection analysis (FIA) enzyme sensor for fructosyl amine monitoring, Anal. Bioanal. Chem. 373 (2002) 211–214.
[24] H.C. Chien, T.C. Chou, Glassy carbon paste electrodes for the determination of fructosyl valine, Electroanal 22 (2010) 688–693.
[25] J. Halámek, U. Wollenberger, W.F.M. Stöcklein, A. Warsinke, F.W. Scheller, Signal amplification in immunoassays using labeling via boronic acid binding to the sugarmoiety of immunoglobulin G: proof of concept for glycated hemoglobin, Anal. Lett. 40 (2007) 1434–1444.
[26] Q. Xue, C. Bian, J. Tong, J. Sun, H. Zhang, S. Xia, A micro potentiometric immunosensor for hemoglobin-A1c level detection based on mixed SAMs wrapped nano-spheres array, Biosens. Bioelectron 26 (2011) 2689–2693.
[27] H.H. Chen, C.H. Wu, M.L. Tsai, Y.J. Huang, S.H. Chen, Detection of total and A1c glycosylated hemoglobin in human whole blood using sandwich immunoassays on polydimethylsiloxane-based antibody microarrays, Anal. Chem. 84 (2012) 8635–8641.
[28] J.T. Liu, L.Y. Chen, M.C. Shi, Y. Chang, W.Y. Chen, The investigation of recognition interaction between phenylboronate monolayer and glycated hemoglobin using surface plasmon resonance, Anal. Biochem. 375 (2008) 90–96.
[29] M.M. Richter, Electrochemiluminescence (ECL), Chem. Rev. 104 (2004) 3003–3036.
[30] W.J. Miao, Electrogenerated chemiluminescence and its biorelated applications, Chem. Rev. 108 (2008) 2506–2553.
[31] L. Hu, G. Xu, Applications and trends in electrochemiluminescence, Chem. Soc. Rev. 39 (2010) 3275–3304.
[32] Q. Liu, J. Huan, A.R. Fei, H.P. Mao, K. Wang, "Signal on" electrochemiluminescence pentachlorophenol sensor based on luminol-MWCNTs @graphene oxide nanoribbons system, Talanta 134 (2015) 448–452.
[33] H. Dai, X.P. Wu, H.F. Xu, M.D. Wei, Y.M. Wang, G.N. Chen, Fabrication of a new ECL biosensor for choline by encapsulating choline oxidase into titanate nanotubes and Nafion composite film, Electrochem. Commun. 11 (2009) 1599–1602.
[34] S. Garcia-Segura, F. Centellas, E. Brillas, Unprecedented electrochemiluminescence of luminol on a boron-doped diamond thin-film anode. Enhancement by electrogenerated superoxide radical anion, J. Phys. Chem. C 116 (2012) 15500–15504.
[35] Y.F. Cheng, R. Yuan, Y.Q. Chai, H. Niu, Y.L. Cao, H.J. Liu, L.J. Bai, Y.L. Yuan, Highly sensitive luminol electrochemiluminescence immunosensor based on ZnO nanoparticles and glucose oxidase decorated graphene for cancer biomarker detection, Anal. Chim. Acta 745 (2012) 137–142.
[36] X.H. Wei, C. Liu, Y.F. Tu, Microemulsion-enhanced electrochemiluminescence of luminol-H_2O_2 for sensitive flow injection analysis of antioxidant compounds, Talanta 94 (2012) 289–294.
[37] J.J. Zhao, W.Y. Guo, J.J. Li, H.H. Chu, Y.F. Tu, Study of the electrochemically generated chemiluminescence of reactive oxygen species on indium tin oxide glass, Electrochim. Acta 61 (2012) 118–123.
[38] L.F. Chen, L.L. Lu, Y. Mo, Z.M. Xu, S.P. Xie, H.Y. Yuan, D. Xiao, M.M.F. Choi, Electrogenerated chemiluminescence of anatase TiO_2 nanotubes film, Talanta 85 (2011) 56–62.
[39] I.S. Grover, S. Singh, B. Pal, The preparation, surface structure, zeta potential, surface charge density and photocatalytic activity of TiO_2 nanostructures of different shapes, Appl. Surf. Sci. 280 (2013) 366–372.
[40] D. Kowalski, D. Kim, P. Schmuki, TiO_2 nanotubes, nanochannels and mesosponge: self-organized formation and applications, Nano Today 8 (2013) 235–264.
[41] W. Zhou, H. Liu, R.I. Boughton, G. Du, J. Lin, J. Wang, D. Liu, J. Mater. Chem. 20 (2010) 1405–1409.
[42] J. Hong, L. Ming, Y.F. Tu, Intensification of the electrochemiluminescence of luminol on hollow TiO_2 nanoshell-modified indium tin oxide electrodes, Talanta 128 (2014) 242–247.
[43] Q. Zhao, C.B. Xiao, Y.F. Tu, The electrochemiluminescence of luminol on titania nanotubes functionalised indium tin oxide glass for flow injection analysis, Talanta 143 (2015) 90–96.
[44] J. Oishi, Y. Asami, T. Mori, J.H. Kang, M. Tanabe, T. Niidome, Y. Katayama, Measurement of homogeneous kinase activity for cell lysates based on the aggregation of gold nanoparticles, Chem. Bio. Chem. 8 (2007) 875–879.
[45] Z.M. Yu, X.H. Wei, J.L. Yan, Y.F. Tu, Intensification of electrochemiluminescence of luminol on TiO_2 supported Au atomic cluster nano-hybrid modified electrode, Analyst 137 (2012) 1922–1929.
[46] X.H. Wei, C.B. Xiao, K. Wang, Y.F. Tu, A nano-TiO_2 supported AuAg alloy nanocluster functionalized electrode for sensitizing the electrochemiluminescent analysis, J. Electroanal. Chem. 702 (2013) 37–44.
[47] H. Dai, Y.W. Chi, X.P. Wu, Y.M. Wang, M.D. Wei, G.N. Chen, Biocompatible electrochemiluminescent biosensor for choline based on enzyme/titanate nanotubes/chitosan composite modified electrode, Biosens. Bioelectron. 25 (2010) 1414–1419.
[48] Y.Y. Lin, H. Dai, G.F. Xu, T. Yang, C.P. Yang, Y.J. Tong, G.N. Chen, Enhanced luminol electrochemiluminescence triggered by an electrode functionalized with dendrimers modified with titanate nanotubes, Microchim. Acta 180 (2013) 563–572.
[49] R. Wang, J. Di, J. Ma, Z. Ma, Highly sensitive detection of cancer cells by electrochemical impedance spectroscopy, Electrochim. Acta 61 (2012) 179–184.
[50] X.L. Chen, W. Liu, L.L. Tang, J. Wang, H.B. Pan, M. Du, Electrochemical sensor for detection of hydrazine based on Au@Pd core-shell nanoparticles supported on amino-functionalized TiO_2 nanotubes, Mater. Sci. Eng. C 34 (2014) 304–310.
[51] D.R. Walt, V.I. Agayn, The chemistry of enzyme and protein immobilization with glutaraldehyde, Trac-Trend Anal. Chem. 13 (1994) 425–430.
[52] Morris Reichlin, Use of glutaraldehyde as a coupling agent for proteins and peptides, Methods Enzymol. 70 (1980) 159–165.
[53] G. Guilbault, Analytical Uses of Immobilised Enzymes, Dekker, New York, 1984, p. 130.
[54] W.Y. Guo, J.L. Yan, Y.F. Tu, The intensification of luminol electrochemiluminescence by metallic oxide nanoparticles, Sci. China Chem. 54 (2011) 1640–1644.